


Attraction between like-poles of two magnets mediated by a soft ferromagnetic material

Tarcísio N. Teles¹, Thiago V.P. de Araújo¹, Yan Levin^{*2}

¹Universidade Federal de Ciências da Saúde de Porto Alegre, Laboratório de Física, 90050-170, Porto Alegre, RS, Brasil.

²Universidade Federal do Rio Grande do Sul, Instituto de Física, 91501-970, Porto Alegre, RS, Brasil.

Received on July 14, 2024. Revised on July 23, 2024. Accepted on July 28, 2024.

We present an engaging educational demonstration designed to captivate students' attention. The experiment reveals an intriguing phenomenon – a surprising attraction between two magnets with identical poles facing each other when a steel metal sphere is inserted between them. Our exploration focuses on both qualitative and quantitative aspects of this magnetic interaction. Specifically, we examine the interaction between two neodymium cylindrical magnets with the like poles facing each other. The experimental setup we introduce allows for the precise measurements of the magnetic force between the magnets. To gain a quantitative understanding of our measurements, we employ electromagnetic theory. This theoretical framework allows us to determine the magnetic energy within the system and to easily calculate the force between the magnets.

Keywords: Magnets, Green function, magnetic field.

1. Introduction

The phenomenon of magnetism has fascinated humans for centuries. It all began with the discovery of magnetite, a natural magnetic iron ore ($\text{FeO-Fe}_2\text{O}_3$), and the lodestone, a naturally magnetic rock that behaves like a compass. The Greeks were the first to study these intriguing materials, and their influence on the study of magnetism persisted for nearly 23 centuries after the initial discovery around 800 B.C. [1–3]. One of the earliest insights into magnetic induction was provided by the Roman poet Lucretius Carus. He eloquently described this phenomenon, but lacked a comprehensive explanation for it, as the concept of magnetic poles was yet to be discovered [4].

The birthplace and date of the first magnetic invention, the compass, remain a matter of historical debate. Some argue that it was developed in China between 2637 B.C. and 1100 A.D., while others suggest that it arrived in China in the thirteenth century A.D., possibly with Italian or Arab origins [5]. Regardless of its origins, the compass had reached Western Europe by the 12th century A.D., bringing with it immense utility and fascination. Albert Einstein himself recalled the profound impact the compass had on him as a child [6].

Presently, easy access to powerful magnets is owed largely to the advancements such as documented in the references [7, 8]. The availability of cost-effective neodymium-based commercial magnets, capable of generating substantial magnetic fields, allows us to use these in physics courses to easily demonstrate the fundamental

principles of electricity and magnetism. Some years ago, we published in a simple quantitative model of electromagnetic braking [9]. This has become a standard demonstration in advanced physics courses – when a strong neodymium magnet falls through a copper pipe, it appears as if it is moving through a dense viscous fluid. The demonstration is a remarkable introduction to Lenz's and Faraday's laws of electromagnetic theory, and never fails to capture the attention of students and professors alike. Surprisingly, one can perform an analytical calculation to predict the velocity of a falling magnet, which is in excellent agreement with the experimental measurement and is sufficiently simple to be presented in an undergraduate Electricity and Magnetism course [9]. For graduate students, one can also explore the dynamics of a magnet falling through an ideal superconducting pipe [10].

In the present paper, we address a different demonstration of electromagnetic theory, which is equally designed to capture student's attention and introduce them to a very important concept of image charges. Consider two magnets: clearly they attract when opposite poles face each other, and repel otherwise. Now, suppose that in the later configuration (like-poles facing each other), a steel metal sphere is inserted between the two magnets. Will the interaction remain repulsive? The answer is: "It depends!" on the distance between the magnets and on sphere's radius.

This is schematically demonstrated in Figure 1, where the arrows show the direction of the force felt by the upper magnet. To quantitatively measure the force between the magnets, a precision scale can be used, as depicted in Figure 2 below. The bottom magnet is placed

*Correspondence email address: levin@if.ufrgs.br

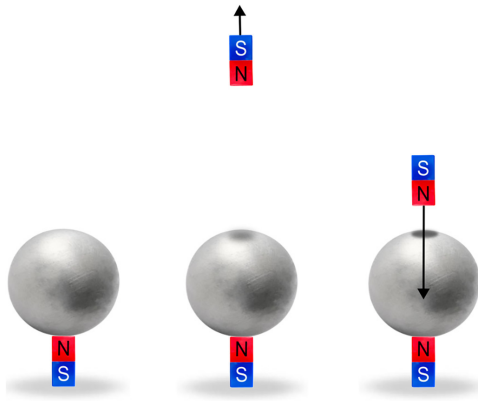


Figure 1: The illustration represents the theoretical framework of the experiment, displaying a magnet attached to the metal sphere on the left, with a second magnet approaching from infinity. Upon the closer approach of the second magnet, repulsion manifests between the two magnets, gradually transitioning to attraction at shorter distances.



Figure 2: The figure depicts the experimental setup, capturing the shift from repulsion to attraction. In the left panel, the baseline condition shows no second magnet, setting a zero tare on the balance. As the second magnet approaches, the balance records an increase due to a repulsive force (central panel). At closer distances, the force transitions into attraction, indicated by a negative scale reading (right panel). It's important to note that the balance scale readings represent authentic experimental data, while the scaled pen with the magnet at its lower extremity serves as a ruler to measure distance, see also Fig. 3.

on top of the scale, with a metal sphere stuck to it. In order to more easily manipulate the second magnet, we placed it into one end of a plastic tube on which we have printed a millimeter scale. In practice we used the plastic cover of a ball-point pen, into which the magnet fits perfectly, see Fig. 3. The repulsive force is indicated by a positive reading on the scale and attractive force by a negative reading on the scale. We can clearly see the change in the sign on the digital display, as the upper magnet approaches the metal sphere.

Due to its simplicity, this experiment is suitable even for a high school course. The unexpected behavior can be particularly intriguing, prompting students to question why the magnets repel at large separations and suddenly begin to attract at short distances. This counterintuitive aspect of the experiment not only sparks critical thinking, but also has the potential to inspire

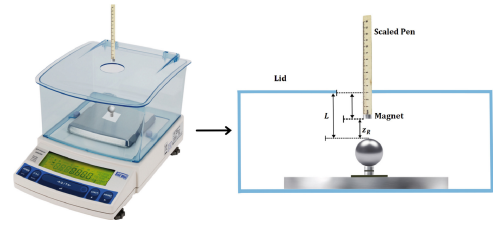


Figure 3: A schematic representation of the experiment. A tube with a millimeter scale (plastic cover of ball-point pen), with magnet at the lower end, is employed to measure the distance z_R between the magnet and the sphere. The bottom magnet is firmly attached to the scale using a double-sided tape.

younger students to pursue physics and science more passionately.

2. Theory

To quantitatively comprehend the physics behind the curious experimental observations, we use Maxwell's equations. Since the studied phenomenon does not involve dynamics, we can focus solely on the magneto-static equations:

$$\vec{\nabla} \cdot \vec{B} = 0, \tag{1}$$

$$\vec{\nabla} \times \vec{H} = \vec{0}. \tag{2}$$

Here, \vec{H} denotes the magnetic field and \vec{B} represents the magnetic induction, which encompasses the effects of magnetic field and the response of the medium through its magnetization \vec{M} ,

$$\vec{B} = \mu_0(\vec{H} + \vec{M}), \tag{3}$$

where μ_0 is the magnetic permeability of the free space.

When a linear and isotropic medium is exposed to magnetic field of intensity \vec{H} , it develops a magnetization \vec{M} in such a way that the magnetic induction is given by

$$\vec{B} = \mu \vec{H}, \tag{4}$$

where μ is the magnetic permeability of the medium [2]. The relationship between \vec{B} and \vec{H} is known as the constitutive equation and can be very non-trivial, especially for ferromagnetic materials, for which μ can itself depend on the magnetic field. In such cases, the material exhibits hysteresis [1]. In the present case, the variation of magnetic field is sufficiently small that we can assume a linear relation between \vec{B} and \vec{H} .

Magnetostatic problems are typically less intuitive than their electrostatic counterparts, mainly due to the absence of isolated magnetic monopoles. In the experiment proposed here, we consider a cylindrical magnet of height d and radius r_m . The effective magnetic volumetric charge density is given by $\rho_m(\vec{r}) = -\vec{\nabla} \cdot \vec{M}$ and the magnetic surface charge density is $\sigma_m = \hat{n} \cdot \vec{M}$, where \hat{n} is the unit vector perpendicular to the surface, in

the outward direction [11]. If the magnet is a uniformly magnetized cylinder – with magnetization along the principal axis – the bulk (magnetic) charge density is zero, so that it can be modeled by two oppositely charged disks of (magnetic) surface charge density $\sigma_m = \pm M$, separated by distance d . The magnetic induction outside the magnet is, therefore, identical to that of two charged disks. We can make a further simplification and replace the charged discs by two point (magnetic) charges $Q = \pm\pi r_m^2 M$ separated by the distance d [9].

Equation 2 allows us to define a scalar magnetic potential ϕ_m such that:

$$\vec{H} = -\vec{\nabla}\phi_m, \tag{5}$$

and by substituting this into eq. 3 and using eq. 1, the potential ϕ_m is found to satisfy the Poisson equation:

$$\vec{\nabla}^2\phi_m = -\rho_m, \tag{6}$$

which for a given boundary conditions has a unique solution.

To derive the boundary conditions for ϕ_m , we need to first examine the boundary conditions for both \vec{B} and \vec{H} [11]. Applying the divergence theorem to a pillbox at the interface S between the inner and outer regions and Stokes' theorem to the circuit C , as shown in Fig. 4, we deduce that:

$$(\vec{B}_{out} - \vec{B}_{in}) \cdot \hat{n} = 0, \tag{7}$$

and

$$(\vec{H}_{out} - \vec{H}_{in}) \times \hat{n} = 0. \tag{8}$$

Here, “in” refers to the inside, and “out” refers to the outside of the sphere. Assuming the material is

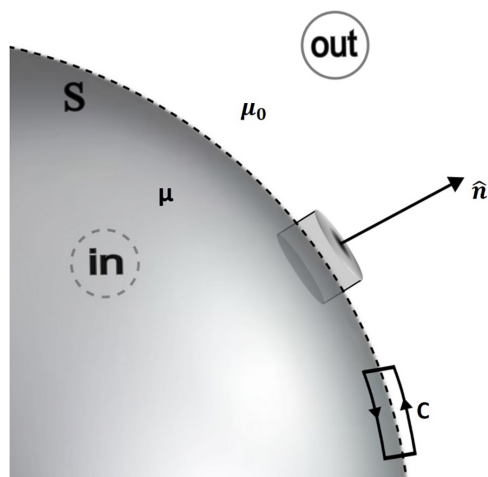


Figure 4: Boundary conditions for the fields \vec{H} and \vec{B} at the interface between the two media. A cylindrical pillbox and a closed circuit, together with the divergence and Stokes theorem, can be used to derive the boundary conditions on \vec{B} and \vec{H} fields, respectively [12]. μ is the magnetic permeability of the medium (sphere), while the magnetic permeability of the air is approximated as μ_0 .

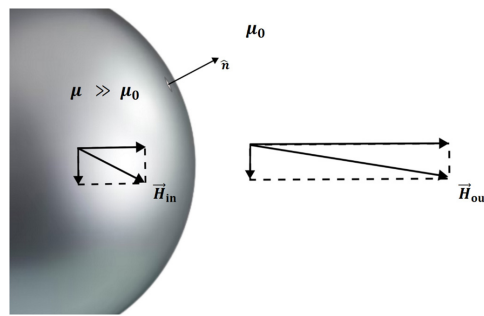


Figure 5: The behavior of the magnetic field \vec{H} between media with different magnetic permeabilities. In the illustrated case, $\mu \gg \mu_0$, resulting in \vec{H} being nearly perpendicular to the surface.

linear and isotropic, we can formulate these boundary conditions in terms of \vec{H} as follows:

$$\vec{H}_{in} \cdot \hat{n} = \left(\frac{\mu_0}{\mu}\right) \vec{H}_{out} \cdot \hat{n}, \tag{9}$$

$$\vec{H}_{in} \times \hat{n} = \vec{H}_{out} \times \hat{n}. \tag{10}$$

It is evident that when $\mu \gg \mu_0$, the normal component of \vec{H}_{out} is much larger than that of \vec{H}_{in} , as illustrated in Fig. 5. Therefore, in the limit $\mu/\mu_0 \rightarrow \infty$, the magnetic field \vec{H}_{out} just outside such material will be perpendicular to its surface, irrespective of the direction of \vec{H}_{in} , except in a special case where \vec{H}_{in} is exactly parallel to the interface.

We observe that in the limit $\mu \gg \mu_0$, the boundary condition for \vec{H} is analogous to that of electric field at the surface of a conductor – the electric field lines are perpendicular to the surface of the conductor. The magnetic permeability of materials like iron and steel, relative to air, typically ranges in the interval $\mu/\mu_0 = [10^3, 10^5]$ [3, 19]. Such high permeabilities enable us to model a magnet near a soft ferromagnetic sphere similarly to an electric dipole near a conducting sphere. Consequently, we can use the methods developed for electrostatics to solve magnetostatics problems for materials with high permeability – for such materials the surface is equipotential, with magnetic field lines normal to it.

Before addressing the problem of two magnets near a sphere, let us consider the case of a single monopole located at position \vec{r}' in front of a ferromagnetic sphere of radius a . The potential generated at the position \vec{r} is determined by the solution of Poisson equation 6 with the boundary conditions given by equations 9 and 10:

$$\vec{\nabla}^2 G(\vec{r}, \vec{r}') = -\delta(\vec{r} - \vec{r}'), \tag{11}$$

where Green function $G(\vec{r}, \vec{r}')$ expresses the potential generated at position \vec{r} by a point charge located at \vec{r}' . The function $G(\vec{r}, \vec{r}')$ can then be used to calculate the potential [12] produced by an arbitrary charge

distribution $\rho_m(\vec{r})$ near a metal sphere:

$$\phi_m(\vec{r}) = \int_V G(\vec{r}, \vec{r}') \rho_m(\vec{r}') dV'. \quad (12)$$

In the case of a single unit charge in front of a conducting sphere, the Poisson equation 11 was solved by William Thompson (Lord Kelvin) in 1848. Kelvin's original solution used the inversion mapping that he developed, which is equivalent to introducing a fictitious charge of strength $-a/r'$ positioned inside the sphere at the "inversion point" located at $(a/r')^2 \vec{r}'$, causing the potential to vanish over the sphere's surface. To ensure that the sphere remains charge neutral, with its surface equipotential, an additional counter-charge of value $+a/r'$ must be placed at the center of the sphere. Subsequently, this method has become known as the "image charge method" (ICM). The ICM is discussed in various undergraduate electromagnetism textbooks, such as those by Griffiths, Reitz, Purcell, and Stump [11, 13–15]. However, when comparing these treatments to more advanced classical works, exemplified by those of Jeans, Maxwell, and Sommerfeld [16–18], as well as more advanced textbooks of Jackson, Landau, Greiner, Stratton, and Panofsky [19–23], the discussion accorded to this very important topic is less than satisfactory. None of the cited references address the problem of a magnet near a ferromagnetic sphere.

Kelvin's solution for the electrostatic potential produced by a unit charge in front of a conducting sphere is:

$$G(\vec{r}, \vec{r}') = \frac{1}{4\pi} \left(\frac{1}{|\vec{r} - \vec{r}'|} + F(\vec{r}, \vec{r}') \right), \quad (13)$$

where the first term is the direct Coulomb potential produced by the unit charge and $F(\vec{r}, \vec{r}')$ is the contribution arising from the image charges:

$$F(\vec{r}, \vec{r}') = -\frac{a}{r'} \frac{1}{|\vec{r} - (a^2/r'^2)\vec{r}'|} + \frac{a}{r'} \frac{1}{|\vec{r}'|}. \quad (14)$$

The first term of F corresponds to the fictitious point charge of magnitude $-a/r'$ located a distance a^2/r' (inversion point) from the center of the sphere, along the vector \vec{r}' . Note that the image charge is always inside the sphere since $r' > a$, as illustrated in Fig. 6. The second term denotes another charge of magnitude $+a/r'$, positioned at the center of the sphere, ensuring that the total charge of the conducting sphere remains zero [13, 19].

Now that we understood the problem of a single charge near a conducting sphere, we can consider the case of four charges, corresponding to the two magnets studied here (see Figures 1 and 6). In this case, the total charge density can be expressed as:

$$\rho_m(\vec{r}) = \sum_{i=1}^4 Q_i \delta(\vec{r} - \vec{r}_i), \quad (15)$$

where for the sake of simplicity, we are considering both magnets to be along the z -axis, with the position of

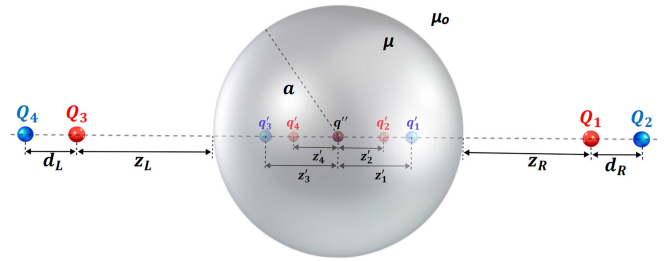


Figure 6: Illustration of the image charge method for two electric dipoles in the proximity of a spherical conductor. In this context, there are two real charges denoted as Q_1 and $Q_2 = -Q_1$ on the right side (R), while another pair of charges, Q_3 and $Q_4 = -Q_3$, are positioned on the left side (L). Their respective vector positions from the center of the sphere are: $\vec{r}_1 = (a + z_R)\hat{z}$, $\vec{r}_2 = (a + z_R + d_R)\hat{z}$, $\vec{r}_3 = -(a + z_L)\hat{z}$, and $\vec{r}_4 = -(a + z_L + d_L)\hat{z}$. The magnitudes of the image charges, indicated with the primes, are specifically $q'_i = -Q_i/r_i$ and differ from one another as these are influenced by both the magnitude of real charges and their position. The image charges are located at the respective inversion points, $\vec{r}'_i = (a^2/r_i^2)\vec{r}_i$ [11, 12]. Since the sphere must remain neutral, with its surface equipotential, we must also place a counter-charge $q'' = -\sum_{i=1}^4 q'_i$ at the center of the sphere. The different colors (online) are indicative of the signs of the charges.

each (magnetic) charge located at: $\vec{r}_1 = (0, 0, a + z_R)$, $\vec{r}_2 = (0, 0, a + z_R + d_R)$, $\vec{r}_3 = (0, 0, -(a + z_L))$ and $\vec{r}_4 = (0, 0, -(a + z_L + d_L))$, while the center of the sphere is at $(0, 0, 0)$. The values of d_L and d_R correspond to the lengths of the left and right magnet, respectively. The monopole charges corresponding to the right and left magnets are respectively: $Q_1 = -Q_2 = Q_R$ and $Q_3 = -Q_4 = Q_L$, as is illustrated in Fig. 6. In the present experiment we will fix the position z_L and move only the right hand magnet.

By analogy with electrostatics, the energy of a system of magnetic charges can be written in terms of $G(\vec{r}_i, \vec{r}_j)$, corresponding to the interaction potential between the two magnetic charges Q_i and Q_j , located respectively at the positions \vec{r}_i and \vec{r}_j , in the presence of an infinitely permeable sphere:

$$U_m = \frac{\mu_0}{2} \sum_{i=1}^N \sum_{j=1}^N Q_i Q_j \left(G(\vec{r}_i, \vec{r}_j) - \frac{\delta_{ij}}{4\pi|\vec{r}_i - \vec{r}_j|} \right), \quad (16)$$

where δ_{ij} is the Kronecker delta. The second term inside the parenthesis subtracts the self energy of each charge. In the specific case under consideration, which involves $N = 4$ charges, the magnetostatic energy is a function of variables: z_L , z_R , d_L , d_R , Q_L , Q_R , and a . The magnetic force is then readily determined by calculating the negative gradient of the energy, eq. 16, with respect to the distance between the magnets:

$$\vec{f}_m = -\vec{\nabla} U_m. \quad (17)$$

This method uses the concept of virtual work that is usually covered in more advanced textbooks on E & M.

Alternatively we can treat the problem analogously to electrostatics, calculating the force acting on the monopoles of the right hand magnet produced by the charges (real and imaginary) through the Coulomb interaction. This method is particularly easy to explain to undergraduate students since it only requires calculating the Coulomb force [14], as illustrated in Fig. 6. For a fixed position of the left-hand magnet, the magnitude of the force on the right-hand magnet is:

$$f_m = \frac{\mu_0}{4\pi} \left(\sum_{i=1}^2 \sum_{j=3}^4 \frac{Q_j Q_i}{|\vec{r}_i - \vec{r}_j|^2} - a \sum_{i=1}^2 \sum_{l=1}^4 \frac{Q_l Q_i}{r_l |\vec{r}_i - \frac{a^2}{r_l^2} \vec{r}_i|^2} + a \sum_{i=1}^2 \sum_{l=1}^4 \frac{Q_l Q_i}{r_l |\vec{r}_i|^2} \right) \quad (18)$$

where the first term corresponds to the force between the real charges $Q_{1,2}$ and $Q_{3,4}$ and the second and third terms are due to the interaction between charges $Q_{1,2}$ and the image and the counter-image charges.

3. Comparison with Experiment

The magnitude of the experimental force was measured directly by reading the value on the balance scale display in kilograms and then multiplying it by the modulus of the acceleration due to gravity (g), which was taken to be 9.8 m/s^2 . This electronic scale is equipped with a cover designed to reduce the impact of air currents on the measurements. We used this cover to gauge the distance between the second magnet and the sphere, using the ruler shown in Fig. 3.

It is essential to note that the natural attraction between the lower magnet and the metallic sphere causes the sphere to be firmly attached to it. On the other hand, since the tray of the electronic balance is not ferromagnetic, the lower magnet needs to be affixed to it by a double-sided tape. To determine the distance between the magnets, we measure the separation between the top of the sphere and the reference point L . Subsequently, using the scaled pen, we measure the distance between the extremity of the upper magnet and the same reference point, $L - Z_R$, see Fig. 3. As the magnet approaches the sphere ($z_R \rightarrow 0$), the force becomes significantly higher, leading to increased fluctuations in the scale readings compared to when the magnets are at greater separations.

We next compare the measured forces with the theoretical predictions, for various distances between the magnets. First, we proceed to determine the values of the charges Q_L and Q_R for a single neodymium magnet. To achieve this, we measure the magnetic induction, denoted as B , at the center of one of the flat circular surfaces of the magnet using a teslameter probe in direct contact with the magnet's surface. By considering that this magnetic induction is generated by two parallel disks – separated by the distance $d_{L,R}$ – each

of radius r_m , carrying a magnetic surface charge density of $\sigma_{L,R} = \pm Q_{L,R}/\pi r_m^2$. The charge of the corresponding monopoles $Q_{L,R}$ is calculated to be [9]:

$$Q_{L,R} = \frac{2\pi B r_m^2}{\mu_0} \sqrt{1 + (r_m/d_{L,R})^2}. \quad (19)$$

The comparison between theory and the experimental data is presented in Fig. 7. We observe an excellent agreement between theory and experiment, without the need for any adjustable parameters. Note that if one would model the cylindrical magnet as a point dipole, one would obtain a very poor agreement with the experimental data. For the smallest metal sphere, we notice a slight deviation between the theory and experiment at short distances. This is primarily due to the failure of the approximation used in the calculation of magnetic energy/force that replaced the disk-like charge distribution of a cylindrical magnet by equivalent point charges. Clearly, when the radius of a ferromagnetic sphere is comparable to the radius of a cylindrical magnet such approximation loses its validity at short separations. Indeed, we see an improving agreement between the theory and experiment for larger metal spheres, see Fig. 7.

We next replace the individual magnets by three neodymium magnets stuck together, and repeat the measurements of the force. Sticking three magnets together does not change the monopole charge, since it is determined only by the magnetization \vec{M} – which remains the same for three magnets stuck together – but will increase the distance between the monopoles. We thus obtain a new set of force curves, which are – once again – in good agreement with the experimental measurements, see Fig. 8.

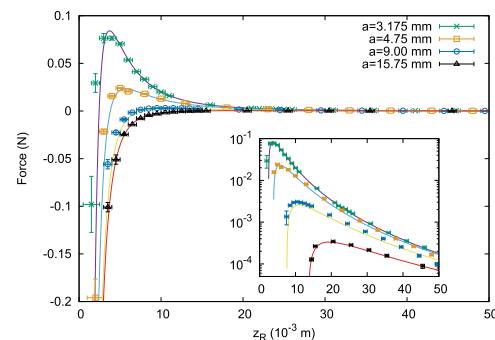


Figure 7: A comparison between theory (curves) and experiment (symbols). Two neodymium magnets of dimensions $d_L = d_R = 3.00(1) \text{ mm}$ and $r_m = 2.50(1) \text{ mm}$ were utilized. The magnetic induction [24] at contact with the flat surface of a magnet was measured using a teslameter [25] to be $B = 0.358(1) \text{ T}$. The curves correspond to ferromagnetic spheres of different radii, a . The position of one magnet was fixed at contact with the metal sphere, while the position of the second magnet z_R was varied. The inset displays the graph on the semi-log scale. There is an excellent agreement between theory and experiment, without any adjustable parameters.

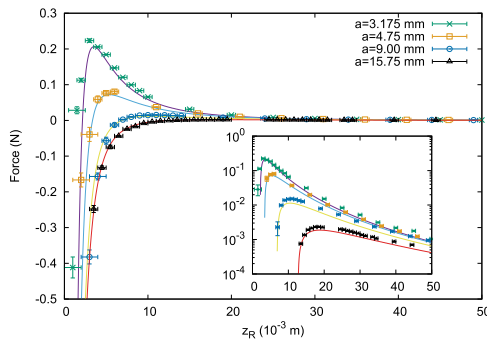


Figure 8: A comparison between theory (curves) and experiment (symbols) when three single magnets are stuck together forming one magnet of length $d_L = d_R = 9.00(1)$ mm. From theory, this corresponds to two monopoles of the same charge as in Fig. 7, but which are now farther apart. Everything else is the same as in Fig. 7. The inset displays the graph on a semi-log scale. Once again there is an excellent agreement between theory and experiment, without any adjustable parameters.

4. Conclusions

Playing with magnets offers an intriguing journey into the realm of electromagnetism. The remarkable agreement between theory and experiment presented in this paper underscores the vast potential of simple demonstrations to capture students' attention and delve deeply into the underlying physics. At a qualitative level, one can understand the physics behind the demonstrations discussed above using the image charge construction. When magnets are far away from the metal sphere, all image charges are located close to the sphere's center, resulting in a negligible contribution to the magnetic induction. This explains why for large separations between magnets – with like-poles facing each other – we only observe repulsion. As the magnets approach the sphere, the image charges located at the two inversion points move closer to the surface. When the magnets are near the surface of the sphere, the interaction with the image charges – which have opposite sign to the charge of the monopoles closest to the surface, leads to an effective attraction between the magnets, a negative force that can be observed in the Figures 2, 7, and 8. The simplicity of this explanation makes it feasible to integrate this demonstration into an undergraduate physics course. The experiment presented in this paper can solidify student's understanding of image charge methods in electrostatic and to show how magnetostatic problems can be approximately solved using electrostatic analogy. Note that in practice it is much easier to use magnets to experimentally demonstrate image charge methods than conductors and electric charges, for which these methods were originally developed. For more advanced E&M course, the problem studied can serve as a gateway to introduce advanced Green function methods, which are very powerful tools in the fields as diverse as

electrical engineering, ionic liquids, and Monte Carlo simulations [26].

Acknowledgments

This work was partially supported by the CNPq and the National Institute of Science and Technology Complex Fluids INCT-FCx. T.N.T. thanks the Laboratório de Ensino de Física at IF-UFRGS for access to the teslameter.

References

- [1] J.F. Keithley, *The Story of Electrical and Magnetic Measurements: From 500 BC to the 1940s* (Wiley, New York, 1999).
- [2] E.T. Lacheisserie, D. Gignoux and M. Schlenker, *Magnetism* (Springer, Boston, 2005), v. 1.
- [3] D.C. Mattis, in: *The Theory of Magnetism I* (Springer Berlin Heidelberg, Berlin, 1981).
- [4] T.L. Carus, *De rerum natura* (Oxford University Press, Oxford, 1984).
- [5] W. Gilbert, *De Magnete* (Gilbert Club/Basic Books, London/New York, 1958), 1 ed.
- [6] P.A. Schilpp (ed.), *Albert Einstein: Philosopher-Scientist* (Open Court, La Salle, 1970).
- [7] M. Sagawa, S. Fujimura, N. Togawa, H. Yamamoto and Y. Matsuura, *Journal of Applied Physics* **55**, 2083 (1984).
- [8] J.J. Croat, J.F. Herbst, R.W. Lee and F.E. Pinkerton, *Journal of Applied Physics* **55**, 2078 (1984).
- [9] Y. Levin, F.L. Silveira and F.B. Rizzato, *American Journal of Physics* **74**, 815 (2006).
- [10] Y. Levin and F.B. Rizzato, *Physical Review E* **74**, 066605 (2006).
- [11] D.J. Griffiths, *Eletrodinâmica* (Pearson Addison Wesley, Boston, 2011).
- [12] K.F. Riley, M.P. Hobson and S.J. Bence, *Mathematical Methods for Physics and Engineering* (University Press, Cambridge, 2006).
- [13] J.R. Reitz, F.J. Milford and R.W. Christy, *Foundations of Electromagnetic Theory* (Addison-Wesley, Boston, 2008.), 4 ed.
- [14] E.M. Purcell, *Electricity and Magnetism* (McGraw-Hill Book Company, New York, 2013), v. 2.
- [15] G.L. Pollack and D.R. Stump, *Electromagnetism* (Addison-Wesley, Boston, 2002).
- [16] J. Jeans, *The mathematical theory of electricity and magnetism* (University Press, Cambridge, 1951), 5 ed.
- [17] J.C. Maxwell *A Treatise on Electricity and Magnetism* (The Clarendon Press, Oxford, 1873).
- [18] A. Sommerfeld, *Electrodynamics: Lectures on theoretical physics* (Academic Press, Cambridge, 1952), v. III.
- [19] J.D. Jackson, *Classical electrodynamics* (Wiley, New York, 1999), 3 ed.
- [20] L.D. Landau and E.M. Lifshitz, *Electrodynamics of Continuous Media* (Pergamon, Oxford 1984).
- [21] W. Greiner, *Classical electrodynamics* (Springer, Boston, 2002).

- [22] J.A. Stratton, *Electromagnetic Theory* (McGraw-Hill Book Company, New York, 1941).
- [23] W.K.H. Panofsky and M. Phillips, *Classical electricity and magnetism* (Addison-Wesley, Boston, 2005), 2 ed.
- [24] F.J. Lowes, *Geophysical Journal International* **37**, 151 (1974).
- [25] PHYWE, *PHYWE Teslameter, digital*, available in: https://www.phywe.com/equipment-accessories/measurement-devices/oscilloscopes/phywe-teslameter-digital_2108_3039/, accessed in: 09/11/2023.
- [26] M. Giroto, A.P. dos Santos and Y. Levin, *The Journal of Chemical Physics* **147**, 074109, (2017).